Time-encoded electrical detection of trace RNA biomarker by integrating programmable molecular amplifier on chip

Gurpreet Kaur, Marcel Tintelott, Mohit Suranglikar, Antoine Masurier, Xuan-Thang Vu, Guillaume Gines, Yannick Rondelez, Sven Ingebrandt, Yannick Coffinier, Vivek Pachauri, et al.

Biosensors and Bioelectronics 257 (2024) 116311

Contents lists available at ScienceDirect

Biosensors and Bioelectronics

journal homepage: www.elsevier.com/locate/bios

Time-encoded electrical detection of trace RNA biomarker by integrating programmable molecular amplifier on chip

Gurpreet Kaur [a,1], Marcel Tintelott [b], Mohit Suranglikar [b], Antoine Masurier [c], Xuan-Thang Vu [b], Guillaume Gines [c], Yannick Rondelez [c], Sven Ingebrandt [b], Yannick Coffinier [b], Vivek Pachauri [b,*], Alexis Vlandas [a]

[a] Institut D'Électronique, de Microélectronique et de Nanotechnologie (IEMN) - UMR CNRS 8520, Univ. Lille Avenue Poincaré, BP 60069, Villeneuve D'Ascq, Cedex, 59652, France
[b] Institute of Materials in Electrical Engineering 1, RWTH Aachen University, Sommerfeldstrasse 24, 52074, Aachen, Germany
[c] Laboratoire Gulliver, Ecole Supérieure de Physique et de Chimie Industrielles, PSL Research University, and CNRS, Paris, France

ARTICLE INFO

Keywords:
Isothermal amplification
BioFETs
Nanowires
ISFETs
miRNA
Cancer
Neurodegeneration

ABSTRACT

One of the serious challenges facing modern point-of-care (PoC) molecular diagnostic platforms relate to reliable detection of low concentration biomarkers such as nucleic acids or proteins in biological samples. Non-specific analyte-receptor interactions due to competitive binding in the presence of abundant molecules, inefficient mass transport and very low number of analyte molecules in sample volume, in general pose critical hurdles for successful implementation of such PoC platforms for clinical use. Focusing on these specific challenges, this work reports a unique PoC biosensor that combines the advantages of nanoscale biologically-sensitive field-effect transistor arrays (BioFET-arrays) realized in a wafer-scale top-down nanofabrication as high sensitivity electrical transducers with that of sophisticated molecular programs (MPs) customized for selective recognition of analyte miRNAs and amplification resulting in an overall augmentation of signal transduction strategy. The MPs realize a programmable universal molecular amplifier (PUMA) in fluidic matrix on chip and provide a biomarker-triggered exponential release of small nucleic acid sequences easily detected by receptor-modified BioFETs. A common miRNA biomarker LET7a was selected for successful demonstration of this novel biosensor, achieving limit of detection (LoD) down to 10 fM and wide dynamic ranges (10 pM–10 nM) in complex physiological solutions. As the determination of biomarker concentration is implemented by following the electrical signal related to analyte-triggered PUMA in time-domain instead of measuring the threshold shifts of BioFETs, and circumvents direct hybridization of biomarkers at transducer surface, this new strategy also allows for multiple usage (>3 times) of the biosensor platform suggesting exceptional cost-effectiveness for practical use.

1. Introduction

Point-of-Care (PoC) bioanalytical or biosensor platforms are positioned to revolutionize diagnostics in environmental, forensics, food safety and personalized healthcare (Blum and Coulet, 2019, Chen and Bashir, 2023). Their ability to label-free detect molecules exceeds the conventional optical-assays based on pre-amplification and labeling techniques (Pachauri and Ingebrandt, 2016; Syedmoradi et al., 2019). In particular, biologically sensitive field-effect transistors (BioFETs) based on low-dimensional transducers such as nanowires (NWs), carbon nanotubes and graphene are demonstrated as efficient platforms for biological and chemical sensing (Kaisti, 2017; Lu et al., 2018; Pachauri et al., 2010). Silicon based BioFET-arrays, especially, due to their high technological readiness for circuit integration and proven methods for surface modification have successfully demonstrated sustained operation and multiplexing capabilities (Gao et al., 2016; Rani et al. 2016, 2020). Even as such nanoscale BioFET-arrays, because of their scalable fabrication, are ideal for integration of advanced quantitative PoC diagnostics, several critical challenges remain for their usage in real conditions (Holzinger et al., 2014). For example, due to operational requirements in biological media, BioFET-arrays face issues related to solid-liquid interface, such as non-specific processes influencing

* Corresponding author.
E-mail address: pachauri@iwe1.rwth-aachen.de (V. Pachauri).
[1] Present address: Bundesanstalt für Materialforschung und -prüfung (BAM), Richard-Willstätter-Straße 11, Berlin, Germany.

https://doi.org/10.1016/j.bios.2024.116311
Received 31 December 2023; Received in revised form 2 April 2024; Accepted 17 April 2024
Available online 24 April 2024

receptor-analyte interaction, large biomolecules creating a charge-screening layer at the interface, biofouling of the interface etc., all of which result in decreased sensitivity and specificity. PoC platforms essentially face serious practical limitations, originating from above mentioned challenges and result in sensor design bottlenecks to achieve technological advancement able to qualify for clinical evaluations. Scientific interests in the development of novel strategies to overcome such challenges and render PoC diagnostics reliable remains very high, as was witnessed during the recent coronavirus disease (COVID) outbreak (Morales-Narvaez and Dincer, 2020). Here, quantitative detection of disease-linked nucleic acids such as miRNAs, cell-free RNAs with relevant clinical concentrations in sub-pico to femtomolar ranges, constitutes a critical PoC diagnostics challenge. Detection strategies for such analytes generally focus on optimizations of biofunctional layers to improve the effective specificity and affinity towards binding of analytes (Borghei et al., 2017; Cheung et al., 2020; Ganguli et al., 2018; Ilkhani and Farhad, 2018; Janegitz et al., 2017; Kong et al., 2015; Lanche et al., 2018; Akhavan et al. 2012, 2014). However, limited success of such strategies require alternative approaches for analyte-specific signal enhancement, that have relied on complex surface modification protocols and operation to achieve any clinical relevance (Dincer et al., 2017; Kelley, 2017; Vu et al., 2019).

For these reasons, current 'gold standard's of such low-concentration biomarkers (miRNAs, cfRNAs) detection are still centered around amplification of the target molecules by quantitative Polymerase Chain Reaction (qPCR) combined with a fluorescent probes (Chen et al., 2015; Nolan et al., 2006; Viljoen et al., 2005). Although PCR-based approaches provide reliable detection, the need for controlled temperature cycling and fluorescent labeling, requiring costly and fragile optics, leads to increased complexity and costs. With the constant advances in technology, alternatives to PCR amplification have been proposed, including isothermal amplification strategies such as LAMP (Loop-Mediated Isothermal Amplification), RCA (Rolling Circle Amplification), EXPAR (EXPonential Amplification Reaction) (Yao et al., 2014). These approaches solve some of the shortcomings of PCR, such as thermocycling, but some significant holdups remain, including an increased propensity of non-specific amplification leading to false positives (Feng et al., 2020). Outbreak of highly contagious COVID-19 once again underscores the urgency for diagnostic platforms with smaller footprints, for which an optimal solution is to make use of sensor chips based on low-dimensional transducers arrays that require minimal sample volumes, can operate at constant temperature and require minimal sample pre-preparation steps. (Morales-Narvaez and Dincer, 2020).

PUMAs, that we integrate with electrical biosensors in this work, are a type of molecular programs (MPs) that via a network of biomolecular circuits, perform complex signal-processing tasks such as bio-oscillators, bio-switches, programmable controllers and neural networks (Chen et al., 2013; Okumura et al., 2022). Such MPs not only open up possibilities to understand cell biology, but also developed innovative strategies for the development of biosensors or molecular robotics using synthetic nucleic acids (Komiya et al., 2019). *In vitro* realization of such biochemical circuits employ synthetic DNA as information encoding molecules owing to its ability to store information, simple base pairing rules, stability and cost-effectiveness (Soloveichik et al., 2010). One such remarkable DNA computing framework is the Polymerase Exonuclease Nickase-Dynamic Network Assembly (PEN-DNA) toolbox, which uses a set of oligonucleotides and enzymes forming a variety of dynamic molecular circuits. Some examples of PEN-DNA toolbox used for detection of DNA or miRNA include three basic steps: (i) selectively identifies the analyte of interest *i.e.* miRNA or DNA, (ii) conversion to another sequence, and (iii) amplifies this sequence with a specific threshold mechanism to prevent unwanted amplification (Gines et al., 2020b) such as shown in Fig. 1. The activation/inhibition reactions in a PEN-DNA toolbox are catalyzed by a set of enzymes including a DNA polymerase, a nickase and an exonuclease. In principle, by adapting the sequence of these oligonucleotide templates, the MP can be adapted for specific targets or conditions promising versatility for detection of multiple targets. However, several concerns persist to employ this technology in real life clinical applications. One of them being the lack of an easy readout platform that, while reducing the dependency on skilled operators, does not compromise on the sensitivity of the biosensor platform.

The novel biosensor strategy as presented in this work integrated PUMA in order to amplify the signal transduction by several orders of

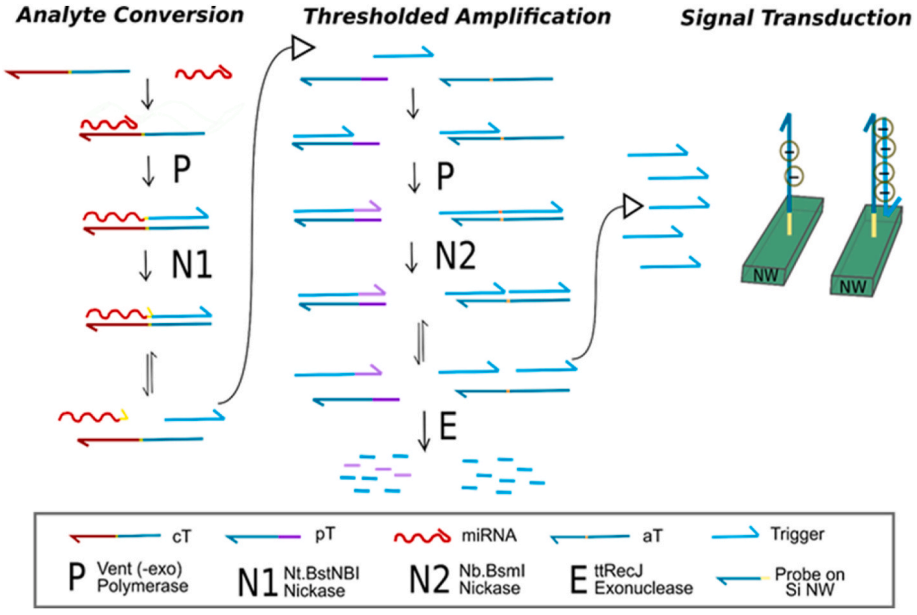

Fig. 1. An overview of the working principle of the Programmable Universal Molecular Amplifier or PUMA based on the PEN toolbox molecular programming approach. It is composed of a converter stage and a thresholded amplifier stage. The former is able to convert a DNA/RNA strand to a trigger tailored for the amplifier. The latter amplifies with a significant gain the molecular signal while preventing false positives using a pseudo template strategy to overcome the system metastable behavior. Finally, the output of the molecular amplifier - a short DNA strand - is detected by via hybridization of PUMA output at the surface of the transducer surface modified with a complementary sequence.

magnitude, improving the output electrical signal significantly and lowering the limit of detection (LOD) so as to match the clinically relevant biomarker concentrations. To the best of our knowledge, only a few examples in literature describe integration of an isothermal amplification process together with an electrical or electrochemical read-out system. One of them concerned the real-time amplification and detection of DNA used for detection of single nucleotide polymorphism from P450 Cytochrome variants (Toumazou et al., 2014). However, the sensor performance of this BioFET based biosensor platform was limited by operation in a low ionic-strength buffer for its pH change based monitoring (Toumazou et al., 2013). Also, upon such pH variation, enzymes (*e.g.* polymerase) should maintain their activity while performing amplification of oligonucleotides. A second example, an integrated LoC biosensor able to electrochemically detect RNA and serological host antibodies from saliva and blood samples from SARS-CoV-2 positive patients (Najjar et al., 2022). The combination of LAMP with electrochemical CRISPR-Cas12a for implementing high sensitivity and high specificity detection strategy, however, required tedious sample preparation steps. The current work focuses on detection of a miRNA biomarker Let7a, which is dysregulated in several types of cancers including breast, lung, prostate, leukemia (Chen et al., 2022) and colon and is known to be down-regulated in Parkinson's disease (Chen et al., 2018; Chirshev et al., 2019). The unique integration of the high sensitivity BioFET-arrays based on Silicon nanowires (Si-NW) with the leak-free isothermal PUMA in a time-encoded approach is demonstrated to carry out routine detection of low concentration miRNA in complex physiological matrices.

2. Material and methods

2.1. Reagents and chemicals

All oligonucleotides were purchased from Integrated DNA Technologies, Inc. (IDT) with HPLC purification and suspended/diluted in Tris-EDTA buffer (or in nuclease-free water when required) and are summarized in Table S1. Template sequences were protected from degradation by the exonuclease enzyme by use of 5' phosphorothioate modifications. Vent(exo-) DNA polymerase. Nt.BstNBI and Nb.BsmI nicking enzymes and bovine serum albumin (BSA) were purchased from New England Biolabs (NEB). A 10-fold dilution of the Nt.BstNBI used throughout the experiments was prepared by dissolving the purchased stock in diluent A (NEB) supplemented with 0.1% Triton X-100. Gibco Fetal Bovine Serum (FBS) was purchased from Fisher and a 10% solution (v/v) was prepared in deionized (DI) water to simulate the physiological concentration. All other chemicals were purchased from Sigma Aldrich and used as received.

2.2. Preparation of reaction mixture

The reaction buffer is composed of 20 mM tris-HCl (pH 7.9), 10 mM $(NH_4)_2SO_4$, 10 mM KCl, 50 mM NaCl, 2 mM $MgSO_4$, 6 mM $MgCl_2$, 100 μM each deoxyribonucleoside triphosphate (dNTP), 0.1% (w/v) Synperonic F 104, 2 μM netropsin and BSA (200 μg/ml). The concentration of templates was fixed as follows: aT 50 nM, cT 0.5 nM, rT 50 nM, pT 10 nM (optimized). After addition of the templates to the reaction buffer and subsequent homogenization, the enzyme mixture was added which consisted of Nb.BsmI (300 U/ml), Nt.BstNBI (10 U/ml), Vent(-exo) (80 U/ml) and ttRecJ. The mixture was divided into aliquots and spiked with different miRNA concentrations. For the control experiments, the same mixture was freshly prepared without (1) the miRNA and (2) cT. The samples (10 μl volume) were then incubated in a qPCR thermocycler (CFX Bio-Rad) for real time fluorescence measurements at 50 °C. For the electrical measurements, the mixture was incubated in the microfluidic chamber assembled over the BioFET-array chips.

2.3. Programmable universal molecular amplifier (PUMA)

The operation of the PUMA molecular circuit can be described in three steps: conversion of the analyte, thresholded amplification and signal transduction. The role of the converter template (cT) is to recognize the target miRNA and convert it into trigger strands *via* polymerization and nicking reactions using a polymerase and a nickase, respectively. The cT is a dual sequence with a nicking site separating the two parts. Once the target miRNA binds to this template, it is elongated by the polymerase and cleaved by the nickase (upon dehybridization), thus producing new trigger strands, which in turn bind to the autocatalytic template (aT). aT is a dual-repeat sequence responsible for the amplification of the trigger strand by similar polymerization and nicking cycles, thereby producing multiple copies of the trigger strand. Exponential amplification however is prone to leaks, *i.e.* non-specific amplifications occur even in the absence of input trigger strands over time. To avoid this self-start, a fixed concentration of pseudo template (pT) is introduced which is fully complementary to the trigger strand on its 3′ end. The aT is trimmed by 2 nucleotides to reduce its affinity towards the trigger (Montagne et al., 2016). The pT is designed such that the last few nucleotides are not complementary to the trigger strand and it lacks a nicking site. As a result, after hybridization of the trigger, extension by the polymerase, and release, the newly elongated strand cannot trigger an aT template, nor can it be cleaved thus removing it from the amplification cascade. This neutralization is controlled by the ratio of aT/pT such that after a certain point (fixed by pT concentration), this reaction is saturated and amplification occurs. An exonuclease is also added to the system to degrade the input and output strands, keeping the system out of equilibrium and in a dynamic state. The templates are protected against this degradation pathway by using 5' phosphorothioate modifications.

Two modes of PUMA functioning have been performed within this study. The first one was carried out to optimize experimental conditions, where a reporter template (rT) captures the amplified trigger strands to provide a real time fluorescent signal read by PCR instrument. The rT consists in a hairpin-shape probe with a FAM fluorophore on its 5′ end and conjugated to a BHQ1 quencher on the 3' end such that fluorescence is observed only when the beacon is in an open configuration upon hybridization with the trigger strands and elongation by the polymerase.

The second mode was to realize the direct electrical readout of the *in situ* amplified trigger strands from the PUMA captured by the complementary strand immobilized over BioFET-arrays for high sensitivity electrical transduction. The intention is to be able to detect ultra-low concentrations of the target analyte *via* the continuous production of trigger strands such that their final concentration exceeds the detection threshold limits of the electrical readout.

2.4. Fabrication, modification and characterization of nanoscale ISFETs

The BioFET-arrays made of Si NWs were fabricated to enable a dip-chip configuration, which allows measurements in bulk solution, as well as an easy integration of fluidics on top. The sensor chip measured 10 mm in length and 5 mm in width. The detailed nanofabrication process together with surface modification is described in supplementary material (S3 to S5).

3. Results and discussion

In this study, we achieve a fully integrated electrical biosensor incorporating PUMA-based isothermal oligonucleotide amplification with BioFETs in a versatile format while carrying out electrical detection of amplicons in a real time quantitative readout (Fig. 2). The operation of the PUMA is carried out inside the fluidic reservoir assembled on top of the BioFET as illustrated in Fig. 2a and b. This approach presents several advantages over the conventional affinity based detection using BioFETs. First, most of the time, an off-device pre-amplification of

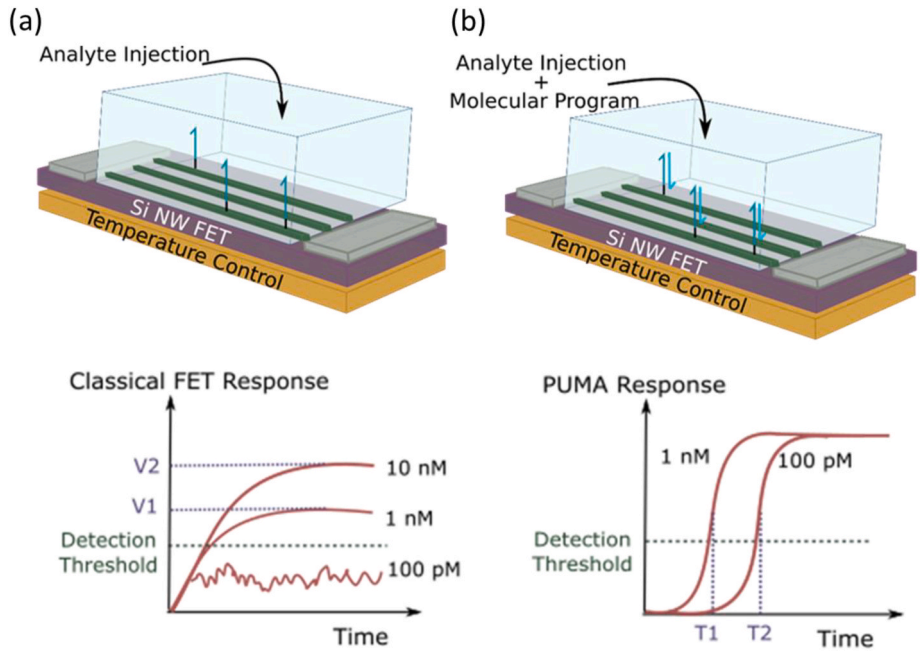

Fig. 2. Integration of PUMA based augmentation of signal transduction for detection of trace biomarkers. On the left side (a), a classical Si-NW based BioFET based detection set-up is shown. The target hybridizes directly with the probe immobilized on the nanowire. The sensitivity is limited by processes and phenomena such as diffusion limited mass transfer at physiological conditions and Debye screening, respectively. The quantitative analysis of the analyte concentration is based on calculating the shift in threshold values (V1 and V2). On the right side (b), this new approach is shown where the target triggers the isothermal PUMA. The PUMA is triggered highly specifically upon the presence of the analyte and generates output of small sequences in an exponential amplification manner. These exponentially amplified output sequences hybridize at the receptor-modified BioFETs in real-time. The effective concentration of PUMA-output sequence concentration reaches about 100s of nM, thereby guaranteeing detection even in complex physiological samples. The initial analyte concentration is no longer encoded in the absolute value of the threshold shift detected but in the time response (T1 and T2) itself thus making quantification more robust.

nucleotide sequences is performed using PCR which is sensitive to interference factors present in complex samples (blood, serum etc.), thus leading to experimental artifact and worse amplification efficacy (Schwarzenbach et al., 2011). In addition, from the perspective of PoC use, the PCR thermocycler requirements are not ideal and thereby giving rise to emergence of isothermal amplification (Feng et al., 2020; Gines et al., 2020a). In addition, in a conventional FET-based biosensor, the quantitative analysis is based on the shift in threshold voltage (V_{th}) of the device, which is subject to drift with respect to ambient conditions and to device-to-device variations. This makes calibration of sensor signals compulsory and prevents the reuse of devices without regeneration of the biofunctional layer. In case of PUMA, a sharp increase of the output sequence concentrations upon the presence of trigger strand leads to a significantly larger shift in threshold voltage. The onset of PUMA-based amplification occurs at different times depending on the initial concentration of the analyte. Owing to this time evolution of the threshold shift due to the amplification in our system, concentration of the target analyte can be interpreted in a time-encoded manner.

We assessed the performance of PUMA based on the PEN-DNA toolbox for the real-time detection of Let-7a miRNA using a standard qPCR instrument using a fluorescence label tagged reporter sequence (Fig. 3). The optimized reaction mixture was spiked with different concentrations of miRNA ranging from 10 fM to 1 nM. The obtained fluorescence intensities were normalized and the fluorescence curves exhibited a typical exponential amplification behavior. miRNA concentrations as low as 10 fM could be detected within a reasonable time duration. The quantification of this real-time detection is carried out in terms of the amplification time (Cq) for various concentrations of miRNA as shown in Fig. 3b. No change in the intensity of the negative control in the absence of target was observed until approximately 175

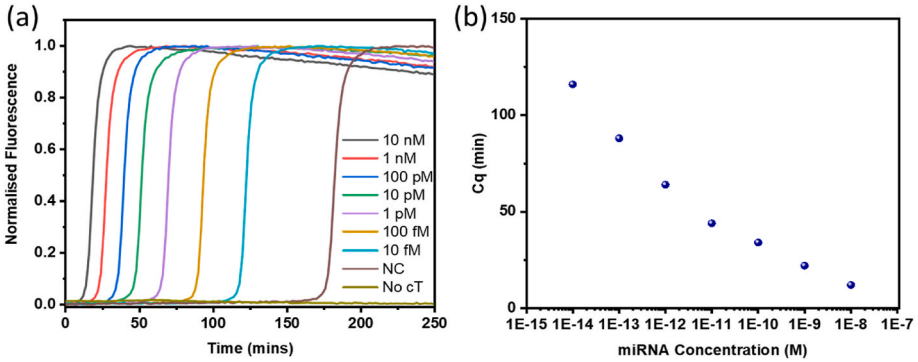

Fig. 3. The PUMA validation was carried out in a real-time PCR thermocycler with various amounts of target RNA ranging from 10 fM to 10 nM and negative controls without miRNA (NC) and without cT (with 10 pM miRNA). (b) The time-based encoding of the initial concentration can be seen on the successive starting times (Cq) of the exponential phase of the amplifier which shows a Limit of Detection under 10 fM.

min. Furthermore, to substantiate the specificity of the molecular program for its target analyte, another control experiment was carried out without addition of the cT in the reaction mixture. Absence of amplification for an extended period suggested that the PUMA is unable to trigger without the cT specific to the target. In order to validate the role of the pT in generating a leak-free mechanism, real time PCR detection of a fixed concentration of miRNA (10 pM) and a negative control was carried out in the presence of different concentrations of pT (Fig. S6). The effect of pT can be clearly seen as the detection of self-start due to non-specific amplifications. For a fixed concentration of miRNA of 10pM, self-start is delayed up to 50 min while increasing pT concentration from 4 to 10 pM (figure S6 a). In the case of negative control, self-start is delayed up to 3 h with increasing concentration of pT from 4 pM to 10 pM (figure S6 b). Beyond this point, which can be tuned, saturation of the leak absorption reaction occurs and amplification initiates even in the absence of target analyte, thus suggesting that the incorporation of a thresholding mechanism through pT is crucial for leak-free operation of the DNA circuit. From this, the best experimental conditions for PUMA were determined for further experiments. In particular, we examined the feasibility of monitoring this reaction using the integrated electrical sensing platform wherein we utilize the BioFETs. First, we carried out the conventional DNA detection using BioFETs to evaluate the LoD. Sensor measurements were performed with various concentrations of trigger DNA using the primary reaction buffer (*i.e.* reaction mixture without the templates and enzymes) added to the microfluidic reservoir on top of the receptor-modified BioFET-arrays. The sample was spiked with increasing concentrations of trigger DNA and the transfer characteristics were examined. The field-effect behavior of BioFETs was analyzed every few mins at a fixed drain-source bias (V_{ds}) of −0.2 V while sweeping the gate voltage (V_g) from −0.8 V to 0 V in steps of −0.05 V. The V_{th} of the BioFET was calculated by plotting the transconductance *vs* Vg and extrapolating the linear portion of the field-effect curve. The BioFETs used here being p-type enhancement mode devices, show no output (*OFF* state) for a given V_{ds} until an accumulation of charge-carriers (holes) occurs in the device channel. Switching them *ON* requires application of a negative bias at the gate, known as the gating-effect. In BioFETs, the gating effect is realized across a solid-liquid interface where an ionic electrical double layer (EDL) forms an electrochemical gate and exerts an electrical double layer capacitance (EDLC) on the device (Pachauri and Ingebrandt, 2016). The change in V_{th} at different concentrations of trigger DNA is represented in supplementary information (Fig. S9). Increase in concentration of the trigger DNA is followed by increased hybridization at the surface of Si NW, inducing more negative charge, thus delineating the shift in Vth. The LoD was assessed and found to be 1 nM. The results are comparable to reports in literature performed in similar high ionic strength solutions (≥100 mM). Once we proved that our BioFET platform is able to detect increasing trigger DNA concentrations, we further study the possibility to follow the dynamic profile of amplification. To do so, an experiment was designed by first employing the autocatalytic exponential amplification of the trigger strands (Fig. 4). The objective of this study was to ascertain the ability of the BioFETs to monitor the amplification and subsequent degradation of the trigger strands. A reaction mixture similar to the one used for PCR was prepared but without miRNA and cT. Instead, a fixed concentration of trigger strand (1 nM) was added to initiate amplification on the aT (50 nM). To check the reversibility of the system using the BioFETs, the concentration of dNTPs or oligonucleotide "fuel" in the mixture was reduced (10 μM) to consume them rapidly and observe the amplification and subsequent degradation of the trigger strands in a shorter time. Fig. 4b illustrates the outcome of this investigation in comparison to the corresponding experiment using the fluorescent readout (Fig. 4a). It can be observed that the ΔV_{th} does not change until approximately 20 min *i.e.* until the amplification initiates. As the autocatalytic template starts amplifying the trigger strands present in the mixture, these strands bind to the complementary DNA strand attached to the BioFET. Further amplification of trigger strands leads to an increase of hybridized DNA and hence, accumulation of negative charge on the BioFET. Consequently, an increase in the density of negative surface charges at the solid-liquid interface translates into lower negative bias at the gate required to switch the BioFET 'ON'. As a result, a shift of field-effect curves towards a positive bias occurred. Next, V_{th} increases before it reaches a maximum where most of the trigger strands are produced and hybridized. It is important to note that since the system is working at 50 °C, the produced trigger strands (melting temperature, T_m ~ 35 °C) are at a temperature higher than their T_m and hence, in a continuously changing state of hybridization and denaturation (Wong and Melosh, 2009). This allows for the monitoring of a time varying concentration of strands in solution as can be seen in Fig. 4. In fact, the molecular circuit is a dynamic system where the produced strands are degraded by the exonuclease, which explains the behavior of V_{th} beyond this point. Indeed, the dNTPs begin to exhaust and the exonuclease degrades the existing trigger strands and V_{th} begins to fall and tends to reach its original value. A similar experiment was carried out in the qPCR thermocycler to investigate the expected behavior of the PUMA. It is interesting to observe that the BioFET's responses are consistent and hence, validated with the real-time amplification in qPCR (Fig. 4a). The time taken for the amplification to commence is nearly the same in both cases, with the BioFETs exhibiting signal change earlier than the qPCR. Both techniques require a sufficient amount of trigger strands to bind to the complementary strand in order to generate an electrical/optical signal. The slight difference in the temporal behavior of PCR and BioFET measurements can be attributed to a number of factors such as variation in temperature control, variation in surfaces in contact with the MP etc. Correspondingly, as the trigger strands become scarce due to degradation and dNTP exhaustion, the optical signal starts to decline, which is

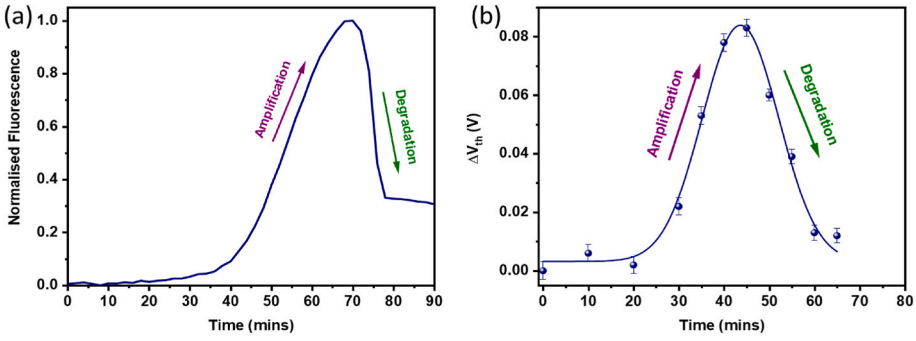

Fig. 4. A comparison of the PUMA based detection followed by (a) standard fluorescence readout performed in a qPCR machine with a total DNA reporting strategy, and (b) BioFET based readout. Here, the molecular program encodes for an exponential amplifier triggered by a 1 nM DNA trigger strand. The amplifier is being run with very little oligonucleotide "fuel" and reaches a peak then decays upon fuel exhaustion. The slight difference in onset time is most likely due to temperature control limitation in the BioFET set-up.

also observed in the electrical response. Further details including the transfer characteristics and the stability of the BioFET platform with time and temperature can be found in the supplementary material (Supplementary Fig. S8). These results support the high potential of this system to successfully detect dynamic amplification and degradation of the trigger strands. Based on that, we then moved to the ultrasensitive detection of miRNA.

To do so, we have thereafter implemented the PUMA system with the BioFETs for the detection of Let-7a miRNA. Supplementary Fig. S7 displays the field-effect curves for the nanoISFET at different time intervals corresponding to the molecular program containing a fixed concentration of Let-7a miRNA. The reaction mixture spiked with 10 pM miRNA was added into the microfluidic chamber over the FET and temperature was set to 50 °C. The transfer characteristics were then recorded every 10 min. Until this point, the Si NW channel is fully depleted of charge carriers and hence, no current flows. Beyond a certain bias at the gate, further accumulation of charge carriers results in electrical conduction, and a measurable drain current I_d output which first increases linearly before attaining a maximum saturation (Poghossian and Schoning, 2014). When the measurements were repeated every 10 min, there was negligible shift in the transfer characteristics suggesting that there is no change in the surface charges at the surface of the BioFET. This behavior was expected owing to the fact that amplification was absent during this time and the single stranded DNA probe attached to the Si NW remained non-hybridized. A very good stability of the DNA immobilized on the BioFET platform together with the absence of electrical device drift at RT and 50 °C and for different times have been confirmed (Supplementary Fig. S7). At around 40 min, a large shift was observed in the characteristics equivalent to a shift in the V_{th}. This can only be accredited to the conversion of Let-7a miRNA into trigger strands followed by their amplification in the PUMA, which in turn binds to the probe DNA probes immobilized on the surface of Si NW. Further, V_{th} continued to decrease for 15 min after which a saturation was achieved.

The response of the PUMA on BioFET has been encoded in time in Fig. 5 and compared with the corresponding measurement in PCR. A control experiment was carried out on the BioFET without the miRNA in solution and the results are also shown in Fig. 5a. The measurements were carried out up to 60 min without any significant shift in V_{th}, as expected since no amplification occurs in the absence of miRNA. We have already seen in PCR measurements that negative control does not amplify for at least 3 h, owing to the pT in solution. It is interesting to observe the agreement between the BioFET and PCR measurements in terms of onset of amplification of trigger stands and the absence thereof (in negative control). This correlation establishes the ability of the PUMA integrated with BioFETs to successfully detect the presence of sub-nanomolar miRNA concentrations and distinguish the signal from a negative control. As expected, this value is lower than the concentration of trigger DNA demonstrated to be detected using a conventional BioFET measurement.

As the PUMA-BioFET platform relies on the hybridization of PUMA-output sequences with the complementary strands functionalized onto the Si-NW surface, two biosensor configurations can be realized: (i) producing the trigger strands via the PUMA separately and introducing them to the BioFET for hybridization, or (ii) a simultaneous production of trigger strands via PUMA and detection by BioFET-array in a single pot. Although the former can address certain technological issues such as heating the BioFETs during sensor operation, the latter is far simpler and easier to implement. Furthermore, the one pot approach gives access to the time-encoded amplification behavior, which is a robust way to establish initial concentration of the analyte of interest. It is important to mention here that this detectable analyte concentration is not the sensor platform's LoD and is merely a concentration chosen to validate the proposed experimental idea and observe the results in a reasonable time. In addition, conventional FET sensors operate at room temperature and it is a well-established fact that the sensitivity of a DNA sensor decreases at temperatures higher than the melting temperature of the DNA strand since a lesser percentage of complementary strands are in a hybridized state at these temperatures.

Here, the PUMA-BioFET system is versatile since we can adapt to concentration changes in the solution due to its dynamic nature as demonstrated by these measurements. In the near future, seamless integration of temperature feedback and control, fluidics set-up, and automated readout towards longer sensor signal recordings will allow us further assessing the capabilities of the novel platform realized here towards the detection of biomarkers with trace concentrations. The fact that the results can be interpreted in time-domain, compensates for any drift in the absolute values of V_{th}, especially in the case of reusability of the devices. Washing steps to regenerate the sensor surface followed by multiple uses tend to shift the absolute value of threshold voltage of the device but such a time encoding can overcome this issue. While other combinations of isothermal amplification and electrical readout have already been reported such as RCA and LAMP with electrochemical detection (Gosselin et al., 2017), they lack the versatility of our approach being unable to easily apply the range of analytes as discussed above and as well to be easily multiplex in a single reservoir. There have been previous attempts to utilize ISFETs for detection of PCR amplified products but these platforms relied on off-chip amplification (Bronder et al., 2018) which make PoC use difficult to implement.

In order to validate the ability of the PUMA-BioFET approach for PoC use with clinically relevant samples, it is imperative to investigate the performance of the platform in a physiological sample. Detection of the target miRNA in such a sample was evaluated by performing the measurements in serum. The PUMA was first performed in PCR with four different FBS dilutions – 1x, ½ x, 1/10x and 1/100x to evaluate the required level of dilution of Fetal Bovine Serum (FBS) for optimal operation (Supplementary Fig. S10). We observed that, although the PUMA operation was hindered in the presence of 1x FBS, higher dilutions yielded an expected PUMA behavior. Consequently, a 10-fold

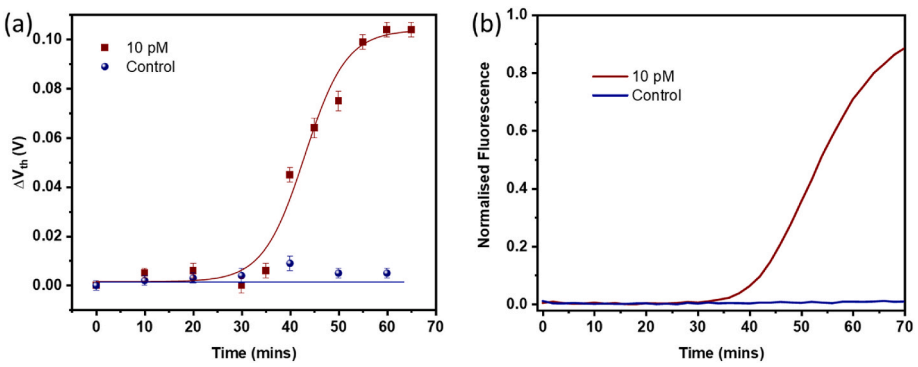

Fig. 5. Operation of PUMA for the detection of miRNA. (a) Time encoded electrical measurements for the PUMA with 10 pM miRNA and negative control (No miRNA) using Si-NW based BioFETs, and (b) the corresponding qPCR measurements.

dilution of the FBS solution (10%) was used as the media for preparing the PUMA, and then spiked with miRNA such that the concentration of miRNA in the final reaction mixture was 10 pM. A control was also prepared simultaneously without using the miRNA. Fig. 6 compares the threshold voltage shift in 10 pM miRNA with the negative control in FBS. The positive sample shows a significant threshold voltage shift validating the possibility to use this detection strategy in clinical samples. The absence of any noticeable shifts in case of the negative control suggests that the PUMA-BioFETs undergo a sustained operation in serum samples without significant risk of biofouling.

It is worth observing that the low-dimensional electrical transducers such as Si-NWs, graphene, etc. often face limitation in performances due to instabilities related to the solid-liquid interface and biofunctional layers, where it is difficult to ensure technological readiness for their successful translation to clinical diagnostics(Kumar et al., 2019). Our PUMA augmented BioFETs strategy here, for being independent from the absolute sensor response of the nanoscale transducer is expected to allow a built in advantage for multiple reuses. To test this, we performed a biosensor measurement 3 times in a row on a single device with a sample rinsing procedure in between the repeats. The V_{th} shift as well as the time at the onset of amplification were monitored (Supplementary Table S2) as in previous experiments. While a significant shift in the absolute V_{th} value was observed with subsequent hybridization and re-hybridization, the shift in V_{th} and, more importantly, the amplification onset time was stable and within the experimental errors. In fact, when PUMA is repeated in qPCR multiple times it gives an error of ± 5 min so the variation observed in the electrical measurements is well within this error. Thereby, we show that the platform can be reused at least 3 times without any significant degradation. It is anticipated that the system is capable of target detection in a complex sample with minimal pre-treatment, for instance cell lysate or waste-water for PoC applications. The LoD was improved by integrating the PUMA giving rise to a leak-proof million-fold molecular amplification. Since the system is isothermal, it is easier to deploy and thanks to the electrical signal readout, it can be miniaturized into a handheld device. The biosensor is capable of multiplexed target (DNA and/or miRNA) detection since the PUMA can be adapted for different analytes by a simple change of the converter template (Gines et al., 2020a).

4. Conclusion

A unique strategy for easy and rapid detection of challenging analytes such as trace miRNA biomarkers is demonstrated by integrating a programmable universal molecular amplifier (PUMA) with BioFET-arrays and establishing a miniaturized biosensor platform. The isothermal PUMA approach presented in this work eliminates background amplification and is extremely versatile, since redesigning the template can reprogram it for any target of interest. The ability of PUMA to perform analyte-specific detection was first established by fluorescent monitoring of Let-7a miRNA down to 10 fM, which is a common biomarker for cancer and neurodegeneration. Then after, the ability of the BioFET platform to follow the amplification and degradation of the molecular signal in real time was confirmed by evaluating the shifts in threshold voltage. We have shown that the platform was stable over long duration at elevated temperatures and was able to detect 10 pM miRNA while differentiating it from the negative control. Let-7a miRNA were successfully converted into trigger strands for subsequent amplification, allowing their electrical detection in physiological buffers and serum samples. The proposed platform holds the potential to be a fully integrated handheld electrical biosensor platform with a simple readout mechanism without compromising on the sensitivity and selectivity for detection of multiple target analytes. In future, the versatility of this system will be explored by applying to detect distinct categories of biomarkers such as signalling proteins, cell-free DNA, other miRNAs etc. and their multiplexing. Further down the line, this system also makes it possible to transduce molecular reaction networks to an electrical signal which upon integration with an electrical to molecular transducer can make a bidirectional communication possible towards realization of biohybrid processors.

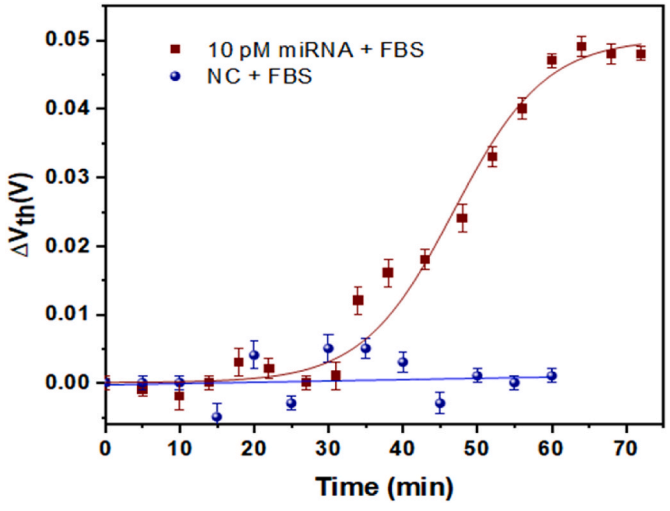

Fig. 6. Si-NW based BioFET readout of 10 pM miRNA (brown curve) and negative control (blue) carried out in Fetal Bovine Serum (10%). The curves are fitted to the time evolution of the PUMA.

Funding information

We acknowledge the Agence Nationale de la Recherche (ANR, France) (Project No. ANR-17-CE18-0031), Deutsche Forschungsgemeinschaft (DFG, Germany (Project No. 391107823 and 440055779) and Deutscher Akademischer Austauschdienst (DAAD) (Project No. 57447131) for generously supporting this research work.

CRediT authorship contribution statement

Gurpreet Kaur: Writing – original draft, Visualization, Validation, Methodology, Investigation, Formal analysis, Data curation. **Marcel Tintelott:** Validation, Methodology, Investigation, Formal analysis, Data curation. **Mohit Suranglikar:** Visualization, Software, Investigation. **Antoine Masurier:** Methodology, Data curation. **Xuan-Thang Vu:** Supervision. **Guillaume Gines:** Validation, Resources, Methodology. **Yannick Rondelez:** Writing – review & editing, Supervision, Resources, Methodology. **Sven Ingebrandt:** Supervision, Resources, Project administration. **Yannick Coffinier:** Writing – original draft, Supervision, Methodology, Investigation. **Vivek Pachauri:** Writing – review & editing, Writing – original draft, Validation, Supervision, Resources, Project administration, Methodology, Funding acquisition, Formal analysis, Data curation, Conceptualization. **Alexis Vlandas:** Writing – review & editing, Writing – original draft, Supervision, Resources, Project administration, Methodology, Funding acquisition, Formal analysis, Conceptualization.

Declaration of competing interest

The authors declare the following financial interests/personal relationships which may be considered as potential competing interests:

Vivek Pachauri reports financial support was provided by German Research Foundation. Alexis Vlandas reports was provided by French National Research Agency. If there are other authors, they declare that they have no known competing financial interests or personal relationships that could have appeared to influence the work reported in this paper.

Data availability

Data will be made available on request.

Acknowledgements

The Renatech Network is acknowledged for providing technical assistance. For microfabrication, technical support by CMNT staff at RWTH Aachen University is gratefully acknowledged. In addition, we thank Jochen Heiss, Dorothee Breuer, Eva-Janina Sekula and Lisa Hertje (all IWE1, RWTH Aachen University) for their help during microfabrication.

Appendix A. Supplementary data

Supplementary data to this article can be found online at https://doi.org/10.1016/j.bios.2024.116311.

References

Akhavan, O., Ghaderi, E., Rahighi, R., 2012. Toward single-DNA electrochemical biosensing by graphene nanowalls. ACS Nano 6 (4), 2904–2916.
Akhavan, O., Ghaderi, E., Rahighi, R., Abdolahad, M., 2014. Spongy graphene electrode in electrochemical detection of leukemia at single-cell levels. Carbon 79, 654–663.
Blum, L.J., Coulet, P.R., 2019. Biosensor Principles and Applications.
Borghei, Y.S., Hosseini, M., Ganjali, M.R., Hosseinkhani, S., 2017. Label-free fluorescent detection of microRNA-155 based on synthesis of hairpin DNA-templated copper nanoclusters by etching (top-down approach). Sensor Actuat B-Chem 248, 133–139.
Bronder, T.S., Jessing, M.P., Poghossian, A., Keusgen, M., Schoning, M.J., 2018. Detection of PCR-amplified tuberculosis DNA fragments with polyelectrolyte-modified field-effect sensors. Anal. Chem. 90 (12), 7747–7753.
Chen, H., Wang, J., Wang, H., Liang, J., Dong, J., Bai, H., Jiang, G., 2022. Advances in the application of Let-7 microRNAs in the diagnosis, treatment and prognosis of leukemia. Oncol. Lett. 23 (1), 1.
Chen, S., Bashir, R., 2023. Advances in Field-Effect Biosensors towards Point-Of-Use Nanotechnology, vol. 34, p. 49.
Chen, L., Yang, J., Lu, J., Cao, S., Zhao, Q., Yu, Z., 2018. Identification of aberrant circulating miRNAs in Parkinson's disease plasma samples. Brain Behav 8 (4), e00941.
Chen, P., Huang, N.T., Chung, M.T., Cornell, T.T., Kurabayashi, K., 2015. Label-free cytokine micro- and nano-biosensing towards personalized medicine of systemic inflammatory disorders. Adv. Drug Deliv. Rev. 95, 90–103.
Chen, Y.J., Dalchau, N., Srinivas, N., Phillips, A., Cardelli, L., Soloveichik, D., Seelig, G., 2013. Programmable chemical controllers made from DNA. Nat. Nanotechnol. 8 (10), 755–762.
Cheung, K.M., Abendroth, J.M., Nakatsuka, N., Zhu, B., Yang, Y., Andrews, A.M., Weiss, P.S., 2020. Detecting DNA and RNA and differentiating single-nucleotide variations via field-effect transistors. Nano Lett. 20 (8), 5982–5990.
Chirshev, E., Oberg, K.C., Ioffe, Y.J., Unternaehrer, J.J., 2019. Let-7 as biomarker, prognostic indicator, and therapy for precision medicine in cancer. Clin. Transl. Med. 8 (1), 24.
Dincer, C., Bruch, R., Kling, A., Dittrich, P.S., Urban, G.A., 2017. Multiplexed point-of-care testing - xPOCT. Trends Biotechnol. 35 (8), 728–742.
Feng, W., Newbigging, A.M., Le, C., Pang, B., Peng, H., Cao, Y., Wu, J., Abbas, G., Song, J., Wang, D.B., Cui, M., Tao, J., Tyrrell, D.L., Zhang, X.E., Zhang, H., Le, X.C., 2020. Molecular diagnosis of COVID-19: challenges and Research needs. Anal. Chem. 92 (15), 10196–10209.
Ganguli, A., Watanabe, Y., Hwang, M.T., Huang, J.C., Bashir, R., 2018. Robust label-free microRNA detection using one million ISFET array. Biomed. Microdevices 20 (2), 45.
Gao, A., Lu, N., Wang, Y., Li, T., 2016. Robust ultrasensitive tunneling-FET biosensor for point-of-care diagnostics. Sci. Rep. 6, 22554.
Gines, G., Menezes, R., Nara, K., Kirstetter, A.-S., Taly, V., Rondelez, Y., 2020a. Isothermal digital detection of microRNAs using background-free molecular circuit. Sci. Adv. 6 (4), eaay5952.
Gines, G., Menezes, R., Nara, K., Kirstetter, A.S., Taly, V., Rondelez, Y., 2020b. Isothermal digital detection of microRNAs using background-free molecular circuit. Sci. Adv. 6 (4), eaay5952.
Gosselin, D., Gougis, M., Baque, M., Navarro, F.P., Belgacem, M.N., Chaussy, D., Bourdat, A.G., Mailley, P., Berthier, J., 2017. Screen-printed polyaniline-based electrodes for the real-time monitoring of loop-mediated isothermal amplification reactions. Anal. Chem. 89 (19), 10124–10128.
Holzinger, M., Le Goff, A., Cosnier, S., 2014. Nanomaterials for biosensing applications: a review. Front. Chem. 2, 63.
Ilkhani, H., Farhad, S., 2018. A novel electrochemical DNA biosensor for Ebola virus detection. Anal. Biochem. 557, 151–155.
Janegitz, B.C., Silva, T.A., Wong, A., Ribovski, L., Vicentini, F.C., Taboada Sotomayor, M. D.P., Fatibello-Filho, O., 2017. The application of graphene for in vitro and in vivo electrochemical biosensing. Biosens. Bioelectron. 89 (Pt 1), 224–233.
Kaisti, M., 2017. Detection principles of biological and chemical FET sensors. Biosens. Bioelectron. 98, 437–448.
Kelley, S.O., 2017. What are clinically relevant levels of cellular and biomolecular analytes? ACS Sens. 2 (2), 193–197.
Komiya, K., Komori, M., Noda, C., Kobayashi, S., Yoshimura, T., Yamamura, M., 2019. Leak-free million-fold DNA amplification with locked nucleic acid and targeted hybridization in one pot. Org. Biomol. Chem. 17 (23), 5708–5713.
Kong, R.M., Ding, L., Wang, Z., You, J., Qu, F., 2015. A novel aptamer-functionalized MoS2 nanosheet fluorescent biosensor for sensitive detection of prostate specific antigen. Anal. Bioanal. Chem. 407 (2), 369–377.
Kumar, S., Kurkina, T., Ingebrandt, S., Pachauri, V., 2019. Graphene based materials for bioelectronics and healthcare. Org. Bioelectron.Life.Sci.Healthc 185–242.
Lanche, R., Pachauri, V., Munief, W.-M., Müller, A., Schwartz, M., Wagner, P., Thoelen, R., Ingebrandt, S., 2018. Graphite oxide electrical sensors are able to distinguish single nucleotide polymorphisms in physiological buffers. FlatChem 7, 1–9.
Lu, X.L., Munief, W.M., Heib, F., Schmitt, M., Britz, A., Grandthyl, S., Müller, F., Neurohr, J.U., Jacobs, K., Benia, H.M., Lanche, R., Pachauri, V., Hempelmann, R., Ingebrandt, S., 2018. Front-End-of-Line integration of graphene oxide for graphene-based electrical platforms. Advanced Materials Technologies 3 (4), 1700318.
Montagne, K., Gines, G., Fujii, T., Rondelez, Y., 2016. Boosting functionality of synthetic DNA circuits with tailored deactivation. Nat. Commun. 7, 13474.
Morales-Narvaez, E., Dincer, C., 2020. The impact of biosensing in a pandemic outbreak: COVID-19. Biosens. Bioelectron. 163, 112274.
Najjar, D., Rainbow, J., Sharma Timilsina, S., Jolly, P., de Puig, H., Yafia, M., Durr, N., Sallum, H., Alter, G., Li, J.Z., Yu, X.G., Walt, D.R., Paradiso, J.A., Estrela, P., Collins, J.J., Ingber, D.E., 2022. A lab-on-a-chip for the concurrent electrochemical detection of SARS-CoV-2 RNA and anti-SARS-CoV-2 antibodies in saliva and plasma. Nat. Biomed. Eng. 6 (8), 968–978.
Nolan, T., Hands, R.E., Bustin, S.A., 2006. Quantification of mRNA using real-time RT-PCR. Nat. Protoc. 1 (3), 1559–1582.
Okumura, S., Gines, G., Lobato-Dauzier, N., Baccouche, A., Deteix, R., Fujii, T., Rondelez, Y., Genot, A.J., 2022. Nonlinear decision-making with enzymatic neural networks. Nature 610 (7932), 496–501.
Pachauri, V., Ingebrandt, S., 2016. Biologically sensitive field-effect transistors: from ISFETs to NanoFETs. Essays Biochem. 60 (1), 81–90.
Pachauri, V., Vlandas, A., Kern, K., Balasubramanian, K., 2010. Site-specific self-assembled liquid-gated ZnO nanowire transistors for sensing applications. Small 6 (4), 589–594.
Poghossian, A., Schoning, M.J., 2014. Label-free sensing of biomolecules with field-effect devices for clinical applications. Electroanalysis 26 (6), 1197–1213.
Rani, D., Pachauri, V., Mueller, A., Vu, X.T., Nguyen, T.C., Ingebrandt, S., 2016. On the use of scalable NanoISFET arrays of silicon with highly reproducible sensor performance for biosensor applications. ACS Omega 1 (1), 84–92.
Rani, D., Singh, Y., Salker, M., Vu, X.T., Ingebrandt, S., Pachauri, V., 2020. Point-of-care-ready nanoscale ISFET arrays for sub-picomolar detection of cytokines in cell cultures. Anal. Bioanal. Chem. 412 (25), 6777–6788.
Schwarzenbach, H., Hoon, D.S., Pantel, K., 2011. Cell-free nucleic acids as biomarkers in cancer patients. Nat. Rev. Cancer 11 (6), 426–437.
Soloveichik, D., Seelig, G., Winfree, E., 2010. DNA as a universal substrate for chemical kinetics. Proc. Natl. Acad. Sci. U. S. A. 107 (12), 5393–5398.
Syedmoradi, L., Ahmadi, A., Norton, M.L., Omidfar, K., 2019. A review on nanomaterial-based field effect transistor technology for biomarker detection. Mikrochim. Acta 186 (11), 739.
Toumazou, C., Shepherd, L.M., Reed, S.C., Chen, G.I., Patel, A., Garner, D.M., Wang, C.J., Ou, C.P., Amin-Desai, K., Athanasiou, P., Bai, H., Brizido, I.M., Caldwell, B., Coomber-Alford, D., Georgiou, P., Jordan, K.S., Joyce, J.C., La Mura, M., Morley, D., Sathyavruthan, S., Temelso, S., Thomas, R.E., Zhang, L., 2013. Simultaneous DNA amplification and detection using a pH-sensing semiconductor system. Nat. Methods 10 (7), 641–646.
Toumazou, C., Thay, T.S., Georgiou, P., 2014. A new era of semiconductor genetics using ion-sensitive field-effect transistors: the gene-sensitive integrated cell. Philosophical transactions. Series A, Mathematical, physical, and engineering sciences 372 (2012), 20130112.
Viljoen, G.J., Romito, M., Kara, P.D., 2005. Current and future developments in nucleic acid-based diagnostics. Applications of Gene-Based Technologies for Improving Animal Production and Health in Developing Countries 211–244.
Vu, C.A., Hu, W.P., Yang, Y.S., Chan, H.W., Chen, W.Y., 2019. Signal enhancement of silicon nanowire field-effect transistor immunosensors by RNA aptamer. ACS Omega 4 (12), 14765–14771.
Wong, I.Y., Melosh, N.A., 2009. Directed hybridization and melting of DNA linkers using counterion-screened electric fields. Nano Lett. 9 (10), 3521–3526.
Yao, J., Yang, M., Duan, Y., 2014. Chemistry, biology, and medicine of fluorescent nanomaterials and related systems: new insights into biosensing, bioimaging, genomics, diagnostics, and therapy. Chem. Rev. 114 (12), 6130–6178.